A HYBRID LES / SGS-PDF COMPUTATIONAL MODEL FOR TURBULENT PREMIXED COMBUSTION

Fernando Oliveira de Andrade, fandrade@aluno.puc-rio.br
Luis Fernando Figueira da Silva, luisfer@esp.puc-rio.br
Pontifícia Universidade Católica do Rio de Janeiro - Department of Mechanical Engineering - Rua Marquês de São Vicente, 225
22453-900 - Rio de Janeiro/RJ, Brazil.

Arnaud Mura, arnaud.mura@lcd.ensma.fr
Laboratoire de Combustion et de Détonique - UPR CNRS 9028 - ENSMA - BP40109 - 86961 Futuroscope, France.

Abstract. *A hybrid Large Eddy Simulation / transported Probability Density Function (LES-PDF) computational model is developed to perform the numerical simulation of variable-density low Mach number turbulent reactive flows. Transport equations for mass, momentum, and scalars are solved together with an equation of state within the LES framework. Turbulence is modeled using the classical Smagorinsky-Lilly closure whereas chemical reaction is first addressed thanks to a global single-step chemistry scheme. The governing equations are discretized using second order accuracy spatial and temporal approximations applied to uniform Cartesian meshes within a finite volume framework. The effects of subgrid scale (SGS) turbulence on the combustion processes are taken into account thanks to a Lagrangian transported PDF model which is coupled with the LES solver. The PDF model relies on the use of a Monte Carlo technique: Stochastic Differential Equations (SDE), equivalent to the Fokker-Planck equations are considered for the progress variable. LES and PDF models are solved simultaneously, exchanging information at each time step, the velocity field, turbulence frequency and diffusion coefficient being provided by LES, whereas the PDF model returns the filtered chemical reaction rate. The resulting computational model is used to perform the numerical simulation of an experimental test case consisting of a CH4-air flame established between two streams of fresh and burnt pilot gases in a constant area square cross section duct. The equivalence ratio in the fresh mixture is 0.8, and turbulent premixed combustion takes place in a regime where a strong interaction between chemical reaction and turbulence is awaited. The numerical solutions provided by the hybrid LES-PDF approach are assessed in terms of both (i) the influence of turbulence on the flame front and (ii) the effects of combustion on the velocity field. The global properties of the turbulent flame, such as the instantaneous and turbulent flame thickness, and the effects of turbulent propagation velocity on the flame stabilization process are also analyzed.*

Keywords*: turbulent combustion modeling, Large Eddy Simulation (LES), subgrid scale Probability Density Function (PDF), numerical simulation*

1. INTRODUCTION

Combustion still remains one of the main sources of energy conversion. The combustion processes are used to provide energy for domestic heating and transportation. Electrical energy is also associated with combustion, when generated in thermoelectrical power plants. Industrial processes, such as the petroleum refinement, the metal treatment and processing, and the cement manufacturing depend heavily on combustion processes as well. By considering these examples, it is clear that the benefits of combustion to the technological development and to the comfort of people are numerous. However, it is important to observe that combustion processes are also associated with environmental issues regarding pollution. The major pollutants resulting from combustion are the particulate materials, the unburned or partially burned hydrocarbons (UHC), the sulfuric oxides (SO_x), the nitrogen oxides (NO_x), and the carbon monoxides (CO) (Law, 2006). In particular, an aggravating environmental problem is the anthropogenic global warming, which is associated with the release of CO_2 in the atmosphere from the oil and coal burning, among other processes. Special attention has been recently paid to the development of alternative and non pollutant mechanisms of energy conversion, such as those associated to the use of solar and wind energy. However, due to the current levels of energy demand and the necessity of large scale production, and considering that the availability of fossil fuels will remain sufficient for decades to come, the changes in the global energetic budget will probably occur slowly and the combustion processes will remain as one of the most important energy conversion processes for many years (WEO, 2008).

Following this scenario, the development of combustion modeling methodologies is crucial, since several advantages can be obtained from the use of numerical simulations to assist in the design of industrial equipments, such as burners, engines and turbines. These advantages include, mainly, the optimization of the combustion processes efficiency and the associated reduction of pollutant emissions.

Usually, turbulent combustion modeling relies on the consideration of partial differential equations that describe the transport of mass, momentum, chemical species mass fractions and energy, coupled with equations of state. The different methodologies to solve this set of equations are the direct numerical simulations (DNS), the simulations based on Reynolds averaged equations (RANS) and the large eddy simulations (LES). Within the DNS framework, the

governing equations are solved up to the smallest time and length scales associated with the turbulence and chemical reaction, without any resort to closure assumptions. Such an approach requires the use of high order precision numerical schemes and the availability of tremendous processing and computational storage capacities, which makes its application usually restricted to oversimplified geometrical configurations and low Reynolds numbers. In RANS a temporal filtering process is applied to the governing equations, which suppresses all the turbulent modes and results in transport equations written for the time averaged flow properties. The influence of turbulence on the mean flow field is determined by the turbulence models. At first sight, LES can be thought as an intermediate framework between DNS and RANS: a spatial filtering process is used to separate the large from the small flow structures. The former are computed explicitly whereas the latter is accounted for through the use of sub-filter turbulence models. It is worth mentioning that, in the present study, a conventional approach has been retained i.e. the LES filter is applied directly in the physical space and the classical box (or top-hat) filter has been retained. Since the behavior of the small scale turbulence is, in general, more isotropic, the LES approach presents the advantage of determining the rate of the energy transfer from the large scale, where the major part of turbulent kinetic energy is contained, to the smallest scales. Therefore, one can reasonably expect the LES to provide much more information about the flow field and its dynamics than the RANS strategy.

In the case of reactive flows, the direct spatial filtering of the chemical reaction rate is often impracticable because the corresponding characteristic scales are too small to be captured at the LES level. As a consequence, the influence of the exothermic chemical reactions on the flow field evolution must be determined thanks to physical models. The most important mechanisms associated with the chemical reactions, such as molecular diffusion, turbulent micro-mixing and heat release, take place at scales that are usually several orders of magnitude smaller than the characteristic mesh size retained to perform the numerical simulations of practical configurations (Pitch, 2006). Nevertheless, LES is a very promising approach for combustion studies because most of reacting flows exhibits strong coherent structures as those encountered for instance when large scale thermo-acoustics instabilities spread out in confined flows (Besson et al. 1999, Guilbert et al. 2008). LES could also lead to an improved description of the turbulence / combustion interactions because, in LES, large structures and instantaneous fresh and burnt gases zones, where turbulence properties differ, are explicitly computed.

With these aspects in mind, the present work describes a hybrid Large Eddy Simulation / transported Probability Density Function (LES-PDF) computational model to perform the numerical simulation of variable-density low Mach number turbulent reactive flows. In this model, transport equations for mass, momentum, and scalars are solved together with an equation of state within the LES framework. Turbulence is modeled using the classical Smagorinsky-Lilly closure (Smagorinsky, 1963), whereas chemical reaction is addressed by means of a global single-step chemistry scheme. The governing equations are discretized using second order accuracy spatial and temporal approximations applied to uniform Cartesian meshes within a Finite Volume (FV) framework. The effects of sub-grid scale turbulence on the combustion process are addressed by means of a Lagrangian transported PDF model which is coupled to the LES solver. The transported PDF model relies on the use of a Monte Carlo technique: Stochastic Differential Equations (SDE), equivalent to the original Fokker-Planck equations are considered for the progress variable. LES and PDF models are solved simultaneously, exchanging information at each time step, the velocity field, characteristic turbulence frequencies and diffusion coefficients being provided by LES, whereas the PDF model returns the filtered chemical reaction rate.

The main objective of the hybrid approach is to combine the LES capabilities that allow to evaluate directly the major part of the turbulent kinetic energy with a transported PDF model to account for the contributions of sub-grid scale chemical reactions. The final aim of the present work is to be able to simulate with a sufficient level of fidelity the most important phenomena involved in the interaction between turbulence and combustion.

The experimental configuration studied by Magre et al. (1988) is used to evaluate the quality of the numerical results obtained with the proposed strategy. The experimental test case consists of a CH4-air premixed turbulent flame established between two streams of fresh and burnt gases in a constant area square cross section channel. In the experiments, premixed turbulent combustion takes place in a regime where a strong interaction between chemical reaction and turbulence is expected. The quality of the numerical solutions provided by the hybrid LES-PDF approach is assessed in terms of both (i) the influence of turbulence on the flame front structure and (ii) the effects of combustion on the velocity field. The global properties of the turbulent flame, such as the instantaneous and turbulent flame thickness, and the effects of velocity propagation on the flame anchoring location are also analyzed.

2. MATHEMATICAL FORMULATION

2.1. Eulerian LES Equations

The reactive mixture is fully described by the chemical species mass fractions, the specific enthalpy, pressure, and the components of the velocity vector. The density is described as a function of the three former variables. The evolution of the reactive flow field is governed by the transport equations of mass, momentum, species mass fractions and enthalpy, coupled with equations of state. In the present work, the following simplifying assumptions are retained:

(a) fluid is considered as Newtonian, (b) body forces, heat transport by radiation, Soret and Dufour effects are neglected, (c) assumptions of unity Lewis number and equal molecular diffusion coefficient for all species are retained, and (d) the model is developed for low Mach number flows. The assumptions regarding the chemical kinetics mechanisms include: (a) global, single-step and irreversible chemical reactions, (b) fuel is the deficient reactant, and (c) null temperature exponent β of the Arrhenius expression. Under the previous set of hypotheses, the species mass fractions and enthalpy transport equations can be written in terms of a single scalar transport equation. The corresponding variable is a normalized temperature, known as progress variable, which is sufficient to evaluate the chemical reaction rate.

In the present work, the retained LES filter is a box filter associated with the uniform Cartesian mesh. Applying a Favre-filtering process on the transport equations of mass, momentum and progress variable leads to (Pope, 2000),

$$\frac{\partial \overline{\rho}}{\partial t} + \frac{\partial \left(\overline{\rho} \widetilde{u}_i\right)}{\partial x_i} = 0, \tag{1}$$

$$\frac{\partial \overline{\rho} \widetilde{u}_i}{\partial t} + \frac{\partial \left(\overline{\rho} \widetilde{u}_i \widetilde{u}_j\right)}{\partial x_j} = -\frac{\partial \overline{p}}{\partial x_i} - \frac{\partial \tau_{ij}^{SGS}}{\partial x_j} + \frac{\partial \overline{\tau}_{ij}}{\partial x_j}, \tag{2}$$

$$\frac{\partial \overline{\rho} \widetilde{c}}{\partial t} + \frac{\partial \left(\overline{\rho} \widetilde{u}_j \widetilde{c}\right)}{\partial x_j} = \frac{\partial}{\partial x_j}\left(\overline{\rho} \Gamma \frac{\partial \widetilde{c}}{\partial x_j}\right) - \frac{\partial Q_j^{SGS}}{\partial x_j} + \overline{S}(c), \tag{3}$$

where u_j are the velocity vector components, ρ is the density, p is the pressure, c is the progress variable, Γ is a diffusion coefficient and S is the chemical reaction rate term. The viscous stress tensor, $\overline{\tau}_{ij}$, is given by,

$$\overline{\tau}_{ij} = \mu\left(\frac{\partial \widetilde{u}_i}{\partial x_j} + \frac{\partial \widetilde{u}_j}{\partial x_i}\right) - \frac{2}{3}\mu \frac{\partial \widetilde{u}_k}{\partial x_k}\delta_{ij}, \tag{4}$$

where μ is the kinematic viscosity, and $\tau_{ij}^{SGS} = \overline{\rho}\left(\widetilde{u_i u_j} - \widetilde{u}_i \widetilde{u}_j\right)$ and $Q_j^{SGS} = \overline{\rho}\left(\widetilde{u_j c} - \widetilde{u}_j \widetilde{c}\right)$ are the sub-grid viscous tensor and the sub-grid progress variable flux, respectively. These terms are modeled according to,

$$\tau_{ij}^{SGS} = -\mu_{SGS}\left(\frac{\partial \widetilde{u}_i}{\partial x_j} + \frac{\partial \widetilde{u}_j}{\partial x_i} - \frac{2}{3}\delta_{ij}\frac{\partial \widetilde{u}_k}{\partial x_k}\right), \tag{5}$$

$$Q_j^{SGS} = -\rho \Gamma_{SGS}\left(\frac{\partial \widetilde{c}}{\partial x_j}\right) = -\rho \frac{\mu_{SGS}}{Sc_{SGS}}\left(\frac{\partial \widetilde{c}}{\partial x_j}\right), \tag{6}$$

where Sc_{SGS} is the sub-grid Schmidt number and μ_{SGS} is the sub-grid viscosity, obtained with the use of the classical Smagorinsky-Lilly model,

$$\mu_{SGS} = 2\overline{\rho}\left(C_S \Delta\right)^2 \left|\widetilde{S}_{ij}\right|, \tag{7}$$

where C_s is the Smagorinsky constant, Δ is the characteristic computational mesh length scale and $\overline{S}_{ij}$ is the resolved rate of strain tensor.

2.2. Lagrangian PDF Equations

The Eulerian transport equation for the sub-grid progress variable PDF, P_c, can be written as (Colucci et al., 1998),

$$\frac{\partial \overline{\rho} P_c}{\partial t} + \frac{\partial \overline{\rho} \widetilde{u}_j P_c}{\partial x_j} + \frac{\partial \overline{\rho}\left(u_j \middle| C - \widetilde{u}_j\right) P_c}{\partial x_j} = -\frac{\partial}{\partial C}\left\{\rho\left[\frac{1}{\overline{\rho}}\overline{\frac{\partial}{\partial x_j}\left(\rho \Gamma \frac{\partial c}{\partial x_j}\middle| C\right)}\right] P_c\right\} - \frac{\partial \overline{\rho} S(c) P_c}{\partial C}, \tag{8}$$

where the third term on the left hand side involves the conditional sub-grid scale velocity fluctuation, and the first and second terms on the right hand side are the conditional micro-mixing and the filtered chemical reaction rate terms,

respectively. The filtered chemical rate appears in a one-point closed form and does not require any special modeling because the progress variable PDF is sufficient to obtain it. Models are required for the two other terms. The sub-grid scale velocity fluctuation is modeled by using the classical gradient diffusion hypothesis (Pope, 1985),

$$\frac{\partial \overline{\rho}\left(u_j \middle| C-\widetilde{u}_j\right)P_c}{\partial x_j} = -\Gamma_{SGS}\frac{\partial P_c}{\partial xj}, \tag{9}$$

and the conditional micro-mixing term is modeled using the IEM model as (Villermaux e Falk, 1994),

$$\overline{\frac{\partial}{\partial x_j}\left(\rho\Gamma\frac{\partial c}{\partial x_j}\middle| C\right)} = \frac{\partial}{\partial x_j}\left(\overline{\rho}\Gamma\frac{\partial \widetilde{c}}{\partial x_j}\right) - \frac{\partial}{\partial C}\left[\Omega_m\left(c-\overline{c}\right)\right], \tag{10}$$

where Ω_m is the turbulent frequency provided by LES. Thus, the final form of the Eulerian progress variable PDF transport equation is,

$$\frac{\partial \overline{\rho}P_c}{\partial t} + \frac{\partial \widetilde{u}_j P_c}{\partial x_j} = \frac{\partial}{\partial x_j}\left[\left(\Gamma+\Gamma_{SGS}\right)\frac{\partial P_c}{\partial x_j}\right] + \frac{\partial}{\partial C}\left[\Omega_m\left(c-\overline{c}\right)P_c\right] - \frac{\partial\left[S(c)Pc\right]}{\partial C}. \tag{11}$$

From a general point of view, for a system described by N thermochemical variables evolving in three spatial dimensions with temporal variations, the joint scalar PDF is a function of (N +3) variables and time (Pope, 1985). As a consequence, the use of either a standard finite difference (FD) or finite-volume (FV) numerical scheme is found to be impracticable. Therefore, to solve the Eulerian PDF transport equation an equivalent particle system is defined such that the particles evolve using SDE in time and space. The evolution in physical space is described by transport equations that use the filtered flow field from the LES solver (Pope, 1985),

$$dx_i = \left[\widetilde{u}_i + \frac{\partial\left(\Gamma+\Gamma_{SGS}\right)}{\partial x_i}\right]dt + \left[2\left(\Gamma+\Gamma_{SGS}\right)\right]^{1/2}dW_i, \tag{12}$$

where x_i is the instantaneous particle position in Cartesian coordinates and dW_i is the corresponding Wiener process, characterized by a Gaussian distribution with zero mean and variance dt, where dt is the current value of the computational time step. Along the progress variable sample space direction, the particles are affected by both mixing and chemical reaction processes (Pope, 1985),

$$dc = \left[\Omega_m\left(\overline{c}-c\right)+S(c)\right]dt. \tag{13}$$

For a sufficiently large number of stochastic particles, the resolution of the system of Eqs. (12) and (13) is statistically equivalent to the solution of the PDF transport equation (11).

2.3. Coupling of the Hydrid Model Solvers

The LES and PDF solvers are coupled by means of a feedback mechanism that exchange information at each integration time step. At the beginning of the simulations the flow field is initialized and the stochastic particles are uniformly distributed in the whole 3-D uniform Cartesian mesh. Balance equations for the mass and momentum, i.e. Eqs. (1) and (2), are first solved within the finite volume framework. The filtered velocity components, the turbulence frequency and the diffusion coefficients are provided to the Lagrangian solver, so that the particles evolution can be evaluated according to the SDE Eqs. (12) and (13). The filtered reaction rate term, evaluated using the Lagrangian representation, then feeds the Eulerian balance equation for the progress variable Eq. (3). In the next step, the transport equation of the progress variable, Eq.(3), is solved, so the temperature field is determined, and the new density field is calculated by means of an equation of state. This procedure is repeated for each integration time step until the end of the simulations.

3. RESULTS AND DISCUSSIONS

3.1. Experimental Test Case

The experimental set-up of Magre et al. (1988) is used to evaluate the numerical results obtained in this work. In this experiment, preheated air enters an admission duct at temperature of 600 K, being later separated into the main and

auxiliary ducts. In the main duct, CH4 is injected immediately upstream of a tabulator, a two-dimensional diaphragm used to homogenize the mixture and generate turbulence, leading to an overall equivalence ratio of 0.8. In the auxiliary duct, CH4 is injected and the mixture is subsequently burned in a combustion chamber, resulting in a pilot flow at temperature of the order of 2,000 K. Both fresh mixture and the burnt gases enter the test section, which consists of a 1,300 mm long channel, with a constant area square cross section of 100 x 100 mm. The fresh mixture enters the upper 80 x 100 mm region, with a mean longitudinal velocity of 65 m/s, and the burnt gases enter the lower 20 x 100 mm with a mean longitudinal velocity of 130 m/s. Even without combustion, this experimental configuration provides very high turbulence intensity, produced by the development of a spatial shear layer and also by the incoming flow velocity fluctuations. In fact, the measured turbulence intensity ranges from 5 to 20%. The estimated turbulence and chemistry characteristic times are of the order of 10μs and 1ms, respectively, leading to an approximate value of the Damköhler number, *Da,* of 0.01. The Kolmogorov length scale and the CH4-air laminar flame thickness are about 0,10 and 0.25 mm, respectively, resulting in a value of the Karlovitz number, *Ka*, of approximately 10. As a consequence, turbulent premixed combustion is expected to take place in the thickened flame regime (Borghi, 1988), which is characterized by a strong interaction between chemical reactions and turbulence.

3.2. Computational Meshes and Boundary Conditions

The computational domain retained to perform the numerical simulations includes the test section entrance up to 800 mm downstream. Three different uniform Cartesian meshes are employed, denoted 500k, 800k and 1600k, consisting of 250x40x50, 320x50x50 and 320x50x100 control volumes in the x, y and z directions, respectively. The governing equations are discretized using a second order central differences scheme and the temporal discretization is achieved by a three time-level scheme (Ferziger e Peric, 2002). The selected time step value is 10 μs, so that the Courant Friedrich Levy (CFL) criteria do not exceed 0.5. The total simulation time is 250 ms, which corresponds to 25,000 numerical iterations. The velocity-pressure coupling is managed by a classical SIMPLEC algorithm. Two different kinds of inflow velocity boundary conditions have been used: (a) mean velocity transverse evolution imposed using a hyperbolic tangent function, and (b) mean velocity transverse evolution typical of a fully developed turbulent channel flow. On both types, normally distributed random fluctuations have been added. Outflow boundary conditions are prescribed by imposing a null longitudinal velocity component derivative and null transverse velocity components. No slip and adiabatic conditions are considered at the channel walls.

3.3. Simulations of Inert Cases

Before running the reactive computations, numerical simulations of inert cases have been performed with three main objectives in mind: (1) preliminary check of the statistical equivalence between the Eulerian and Lagrangian PDF formulations, (2) analysis of both the computational mesh influence and sensitivity to inflow boundary conditions, (3) analysis of the structure of the inert flow, with special emphasis on the turbulence properties.

The equivalence between the Eulerian and Lagrangian PDF formulations are analyzed in terms of the first and second statistical moments of an inert passive scalar. The comparisons are performed at four different cross sections downstream of the test section inlet. The obtained results, not reported here for the sake of brevity, display a quite good agreement between the Lagrangian and the Eulerian formulations: maximum observed discrepancies are lower than 8% in the shear layer region. Since these differences can be related to the number of particles initially distributed in each control volume, used by the Monte Carlo solver, a particle number sensitivity analysis has been also performed using successively 100, 200 and 300 particles initially distributed in each control volume. It is observed that, for this particle number interval, the results obtained for the first and second statistical moments of the inert passive scalar remains almost identical and the agreement is not significantly improved by increasing the number of particle per cell. As a consequence, to reduce the computational costs, the simulations of reactive cases are based on 100 particles initially distributed in each control volume.

The inert flow field analysis demonstrates that, for both inflow boundary conditions, the simplified technique used in this work to generate the inflow turbulent fluctuations results in underestimated levels of turbulence activity just downstream of the test section inlet. The major proportion of the turbulent kinetic energy develops 200 mm downstream from the channel entrance, due to the strong transverse gradients of the mean longitudinal velocity component produced in the shear layer region. It is also found that, outside this region, the calculated Reynolds stresses are considerably lower than those evaluated from the experiments.

The mesh sensitivity analysis shows that the results obtained by the three meshes are practically identical, in terms of the mean longitudinal velocity component and the Reynolds stresses components distribution. Small differences are noted when the spatial development of the shear layer is considered. The mesh 1600k seems to reproduce the beginning of the shear layer growth a little bit further upstream than the other two meshes. Figures 1(a) to (c) show the iso-surface of vorticity magnitude, for $|\omega|=8000\ s^{-1}$, as obtained using the meshes 500k, 800k and 1600k, respectively.

Since the inflow boundary conditions described by a typical mean velocity transverse evolution of fully developed turbulent channel flow resulted in a slightly better agreement with the experimental data in terms of the Reynolds

stresses distribution, and the mesh 1600k provided a better description of the shear layer growth, these parameters are selected for the simulations of reactive cases.

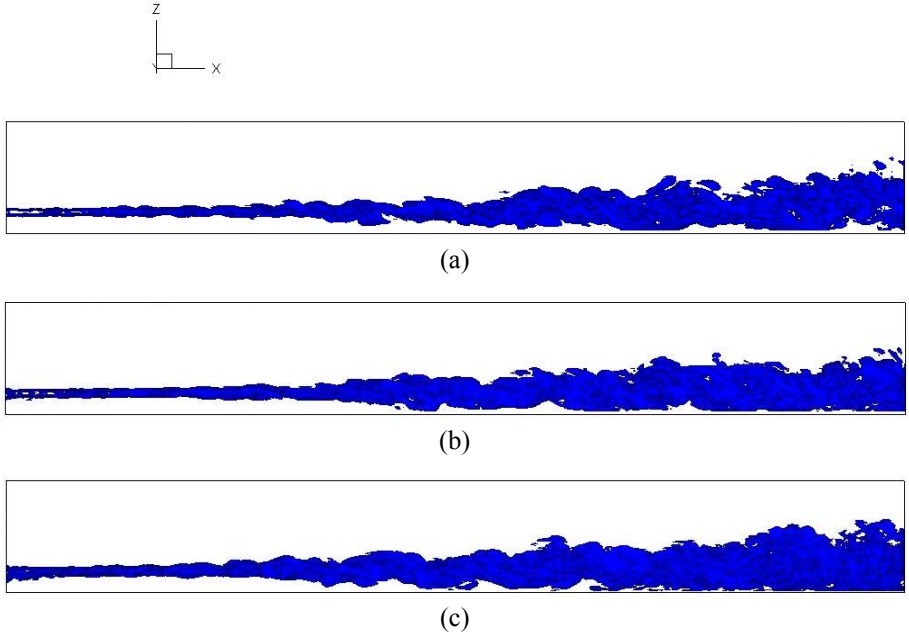

Figure 1. Iso-surface of vorticity magnitude, for $|\omega|=8000\ s^{-1}$: (a) mesh 500k, (b) mesh 800k, (c) mesh 1600k.

3.4. Simulations of Reactive Cases

The simulations of inert cases were crucial to determine the mesh size and the number of particles to be employed in the Monte Carlo solver. Also, the inflow boundary conditions were selected, which consist of typical mean velocity transverse evolution of fully developed turbulent channel flow, superposed by normally distributed random fluctuations. The main duct incoming flow is characterized by a maximum longitudinal velocity of 65 m/s, being the incoming turbulence prescribed by uniform distributed random fluctuations corresponding to 10% of the mean velocity transversal evolution. The auxiliary duct incoming flow presents a maximum longitudinal velocity of 130 m/s, and the incoming turbulence is introduced by uniform distributed random fluctuations corresponding to 20% of the mean velocity transversal evolution. The splitter plate that separates both incoming flows is also represented at the entrance of the computational domain. The inlet progress variable transverse evolution is described by a uniform distribution, where $c= 0$ corresponds to the fresh mixture at temperature $T=T_u= 600$ K and $c=1$ represents the burnt gases at $T=T_b=2000$ K. Figure 2 illustrates the transverse evolution of the mean longitudinal velocity and the progress variable used as the inlet boundary conditions for the simulations of reactive cases.

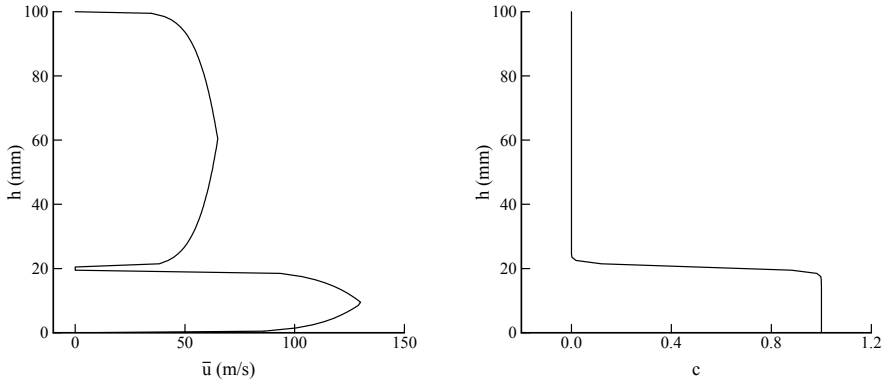

Figure 2. Inlet boundary conditions used in the simulations of reactive cases. Left: transverse evolution of the mean longitudinal component of velocity. Right: transverse evolution of progress variable.

In the reactive cases, the fresh mixture is characterized by a equivalence ratio of 0.8, so that combustion is initiated by the contact of the fresh mixture with the burnt gases at the region immediately downstream of the channel entrance, and develops along the channel length, reaching an anchoring point at the upper channel wall about 400 mm

downstream. The chemical reaction rate is determined by the Arrhenius empirical expression, using an activation temperature of 10,000 K, the fresh mixture temperature of 600 K and the burnt gases temperature of 2,000 K, resulting in,

$$S(c) = 2\rho A 10^3 (1-c)\exp\left(\frac{10{,}000}{600+1400c}\right) \tag{14}$$

where A is the pre-exponential constant, which is inversely proportional to the chemistry characteristic time scale.

Figure 3(a) shows a shadowgraph image of the turbulent flame (Magre et al., 1988), represented by the diagonally distributed darker structures, obtained by the use of high speed film recording at 4,000 frames per second. This figure presents a region between 150 to 350 mm downstream of the test section entrance. It can be seen that the flame structures are wrinkled and distributed by the effects of turbulence on chemical reactions. The flame appears to be in the thickened regime, and according to Magre et al. (1988), features a thickness larger than 10 cm in the direction parallel to the stream lines. It is important to observe that the shadowgraph method provides spanwise integrated information, so the visual thickness is possibly enlarged by the flame wrinkling in the spanwise direction.

Figure 3(b) shows an instantaneous image of the filtered chemical reaction rate calculated by the LES-PDF model, which represents the instantaneous turbulent flame for a region comprehending 100 to 350 mm downstream of the test section entrance. Differently from the spanwise integrated experimental visualization, this image corresponds to a longitudinal plane obtained in the center of the test section. Direct comparisons between the two images can be performed only qualitatively.

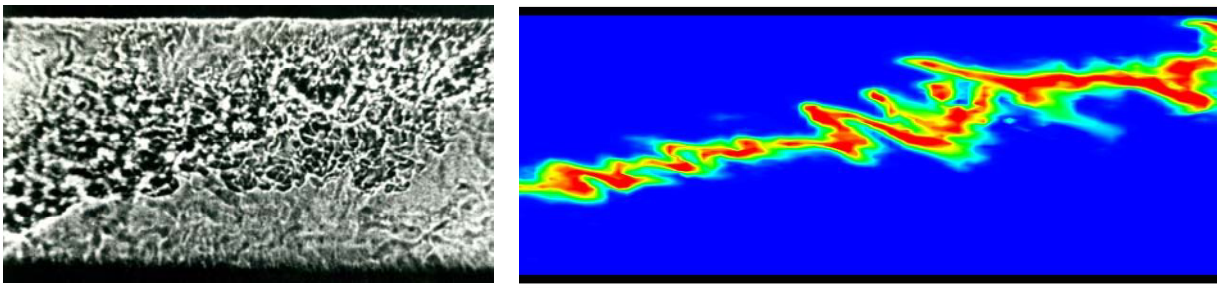

(a) (b)

Figure 3. (a) Instantaneous experimental visualization of the flame front (courtesy of Dr. Roland Borghi), (b) Instantaneous visualization of the flame front, corresponding to the filtered reaction rate calculated by LES-PDF.

It can be seen that the LES-PDF model is capable of representing some effects of turbulence upon the chemical reactions, in particular the wrinkling and stretching of the flame front. In fact, in some regions, pockets of reacting gases are displaced away from the flame front, possibly in the locations of higher turbulent mixing intensity. Some discontinuities in the flame structure are also apparent, which indicate the possibility of local reaction extinction. The thickness of the instantaneous flame ranges from 5 to 10 cm, resulting in a good agreement with the experiments conducted by Magre et al. (1988).

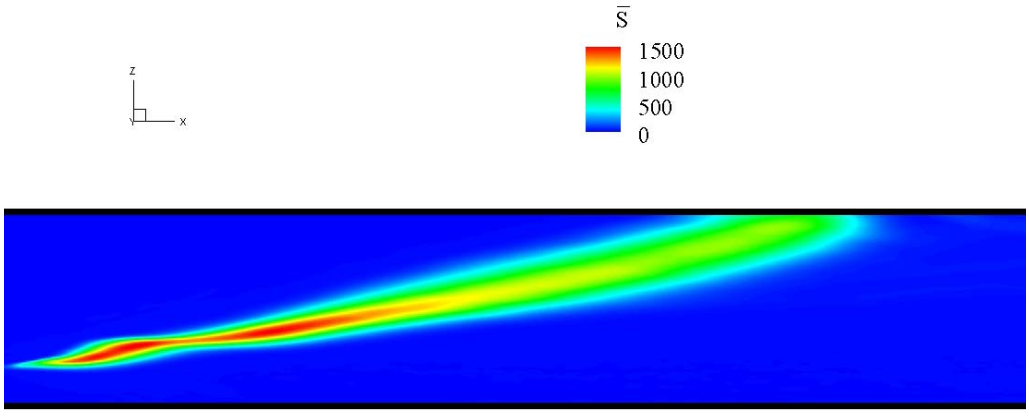

Figure 4. Time averaged chemical reaction rate (turbulent flame brush thickness).

Figure 4 shows the time averaged chemical reaction rate in $kgm^{-3}s^{-1}$, obtained in a longitudinal plane at the center of the test section, and for a region comprising the test section entrance up to 500 mm downstream. Here, the averaged chemical reaction rate corresponds to the mean turbulent flame thickness, or the turbulent flame brush thickness, δ_T. In the experiments of Magre et. al. (1988) it is mentioned that δ_T is approximately 10 cm, measured in the direction parallel to the stream lines. In the present work, δ_T is around 10 cm in $h=50\ mm$, that is, in the middle of the channel height. Higher values are observed toward the upper channel wall and a gradually decrease of the values occur in the direction of the channel entrance.

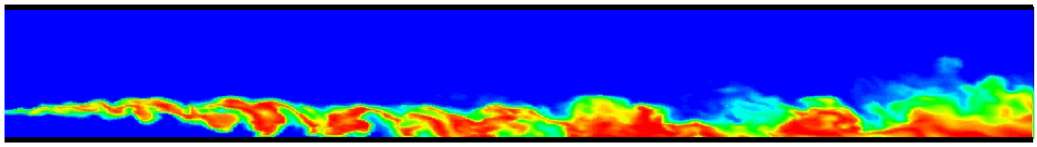

(a) $t = 35\ ms, A=2000, i.e.\ \phi=0.50$

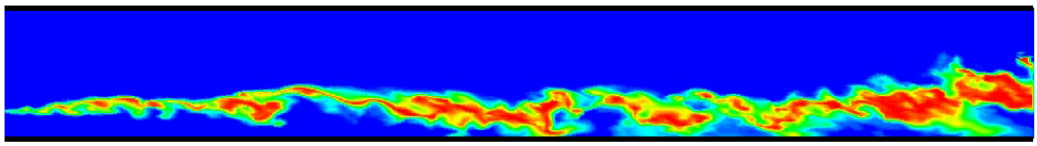

(b) $t = 37\ ms, A=2270, i.e.\ \phi=0.54$

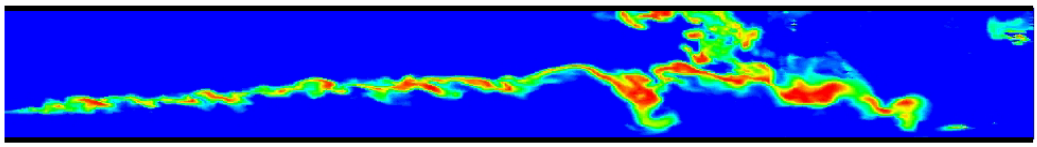

(c) $t = 42\ ms, A=2940, i.e.\ \phi=0.64$

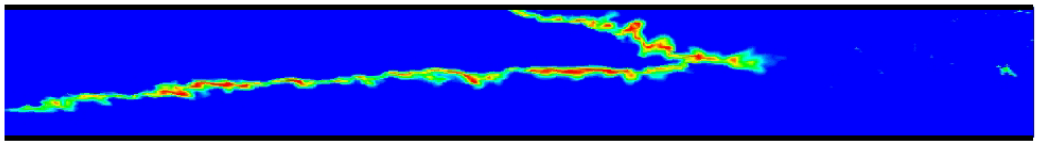

(d) $t = 45\ ms, A=3400, i.e.\ \phi=0.71$

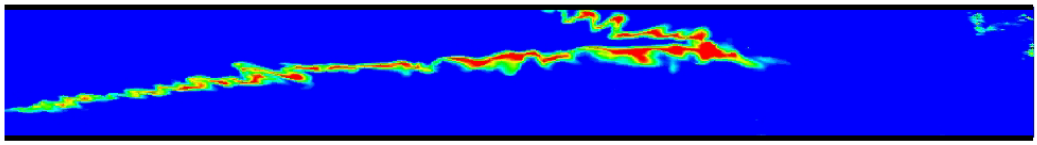

(e) $t = 46\ ms, A=3500, i.e.\ \phi=0.72$

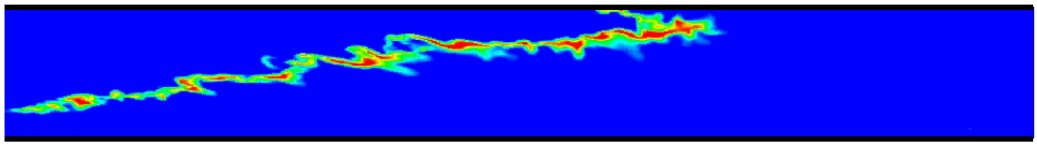

(f) $t = 47\ ms, A=3600, i.e.\ \phi=0.74$

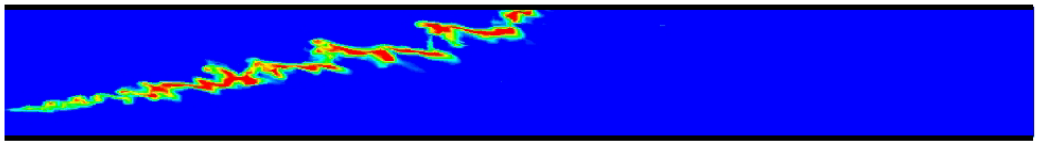

(g) $t = 52\ ms, A=4000, i.e.\ \phi=0.80$

Figure 5. Instantaneous flame front as a function of the equivalence ratio for a longitudinal cross section located in the middle of the channel width.

The interaction between turbulence and chemical reactions are also investigated for different values of the equivalence ratio, ϕ. The simulations start with $\phi = 0$, that is, with the inert flow. At $t=35ms$ a reactive mixture characterized by $\phi = 0.5$ is injected. This value is increased along the simulation up to $\phi = 0.8$ at $t=50$ *ms*, and kept constant until the end of the simulations. This procedure is achieved by linearly increasing the pre-exponential constant of the Arrhenius expression: for $A = 2000$, the equivalence ratio is approximately 0.5 and for $A = 4000$ the equivalence ratio is about 0.8.

Figures 5(a) to (g) show the instantaneous flame front, represented by the instantaneous chemical reaction rate, obtained for a longitudinal plane located in the middle of the channel width, as a function of the equivalence ratio. Figure 5(a) and (b) show that, for low values of equivalence ratio, the flame is positioned practically parallel to the incoming flow. In these cases, the chemical reactions occur on the shear layer developing region, where the turbulence intensity is the highest. For this reason, it is observed that the flames are characterized by large thicknesses, with the maximum values ranging approximately from 15 to 20 cm. It is also seen that the flames are strongly wrinkled and stretched by the turbulent movements.

With the increase of the equivalence ratio, the turbulent flame velocity propagation also increases. Figure 5(c) shows that the flame front bends toward the fresh mixture, advancing firstly in the region near the upper channel wall, where the flow longitudinal velocities are lower when compared to the shear layer region. It can be seen that during this flame front movement, turbulence acts by displacing pockets of reacting gases along the downstream flow.

Figure 5(d) shows a larger inclination of the flame front toward the fresh mixture. It can be seen that the flame is now located completely out of the shear layer influence region. Since in this region the turbulent intensity is lower, the flame front characteristic thickness decreases. However, the strong wrinkling and stretching induced by turbulence are still evident.

Figures 5(e) and (f) show that the flame front angle keeps increasing with respect to the longitudinal channel walls, according to the equivalence ratio increment, and Figure 5(g) illustrates the stabilized premixed turbulent flame, which has an anchor location at the upper wall between 300 and 400 mm downstream of the channel entrance.

In the case of low Mach number flows, most of the influences of combustion on the turbulence properties are due to gases density variations associated to thermal expansion. The energy release from the chemical reactions increases the gases temperature in the flame front region, which leads to volumetric expansions and to consequent decreases of specific mass. In the present work, the temperature gradients at the flame front region result in a density variation ratio between fresh and burnt gases of approximately 3, which may strongly influence the behavior of the mean and fluctuating characteristics of the velocity field.

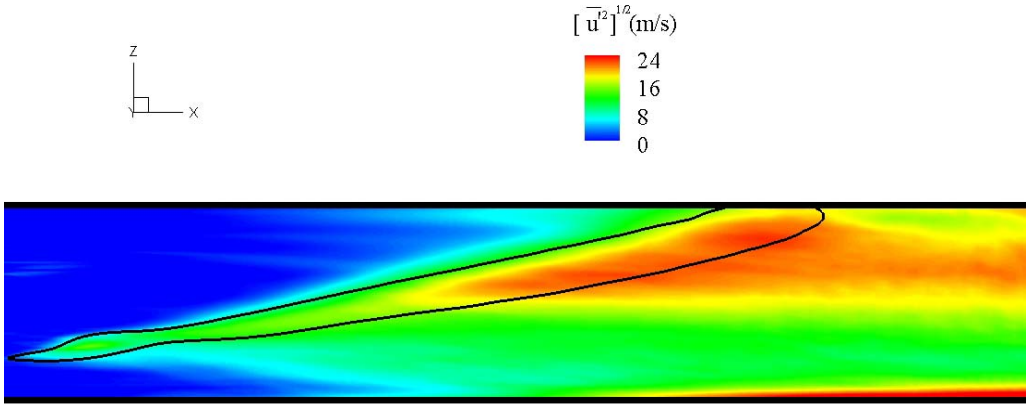

Figure 6. Distribution of the rms of the longitudinal fluctuating velocity component.

Figure 6 shows the rms of the longitudinal fluctuating velocity component, obtained for a longitudinal plane located in the middle of the channel width, and for a region comprising the test section entrance up to 500 mm downstream.
The black line indicates the position of the mean flame brush, corresponding to the time averaged reaction rate. This figure indicates a strong increase of the longitudinal velocity fluctuations in the flame front region, particularly on the upper half of the channel. This increase can be associated with the gases acceleration through the flame front, leading to the rise of the longitudinal components of the fluctuating velocity. It is also observed that the combustion influences on the velocity fluctuations are propagated to the region downstream of the flame front, and smaller fluctuation increases are experienced in the region immediately upstream of the flame front.

Figures 7(a) and (b) show instantaneous images of the lower and upper region of the flame front presented in Figure 3(b), respectively, obtained for a longitudinal plane located in the middle of the channel width, where the flame front is represented by the black lines. The phenomenon known as flame generated vorticity (Peters, 2000) is investigated. The positive vorticity is represented in red color and is associated with a counter-clockwise rotation. The negative vorticity is represented in blue color and is associated to the clockwise rotation relative to the longitudinal cross section.

Both figures suggest the generation of intense vorticity in the flame front region, which can be associated with the gas expansion effects induced by exothermic chemical reactions. The vortices also seem to influence the flame front structure: the superimposition of the black lines that delineates the flame front with the vorticity field suggests that the strong counter-clockwise vortices align with the flame front towards the burnt gases, see Figure 7. On the other hand, the strong clockwise vortices appear to distort the flame front to the fresh mixture direction. Therefore, the combination of these effects contributes to the overall flame stretching, wrinkling and distribution processes. However, it must be emphasized that this analysis is not fully conclusive, since Figures 7(a) and (b) correspond to a single instantaneous image. A complete investigation of the flame generation of vortices and the mutual effects on the chemical reactions would require a set of instantaneous images recorded in sequence in order to identify the coming vortices, the passage of them through the flame front and the resulting effects of the interaction.

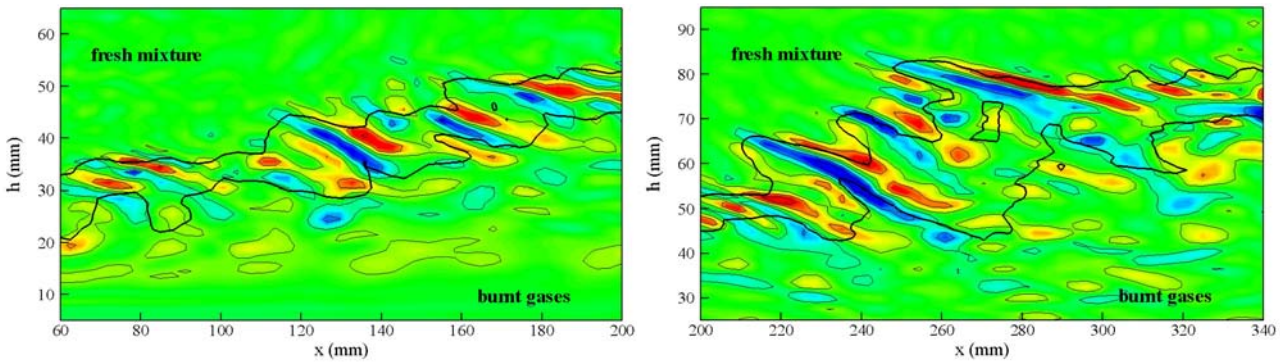

(a) (b)

Figure 7. Vorticity field for the (a) lower and (b) upper instantaneous flame front region.

4. FINAL REMARKS AND FUTURE RECOMMENDATIONS

In the present study, a hybrid large eddy simulation / transported probability density function (LES-PDF) approach has been developed to simulate a case of variable-density low Mach number premixed turbulent combustion, characterized by the existence of intense interactions between turbulence and combustion. The qualitative analysis of the turbulent flame global properties suggests that the methodology is capable of predicting effects of flame stretching, wrinkling and distribution by turbulence. The coupling between turbulent mixing and chemical reactions is described by the probability density function transport equation, which used in the LES framework permits a detailed representation of the interaction between mixing and chemical reaction. The effects of increasing the mixture equivalence ratio are showed by incrementing the Arrhenius pre-exponential constant and the resulting flame stabilization location is in good agreement with the experiments. The calculated instantaneous flame thickness, as well as their average counterparts (i.e. the flame brush thickness), are also well predicted. The effects of combustion on turbulence are evidenced by the high levels of fluctuating longitudinal velocity in the flame front region and by the flame induced production of vorticity. However, further investigations are still required to study quantitatively the influence of combustion on turbulence.

To improve the quality of the results obtained in this work, some modifications in the model are suggested, such as: (a) the use of more sophisticated methods for generating inflow turbulent boundary conditions, such as the ones that take into consideration a more realistic turbulent kinetic energy spectrum, and (b) the use of dynamic type of models to calculate the sub-grid viscosity. For the further steps, it is suggested to include a detailed chemical kinetics description and also to test different micro-mixing models able to describe thickened flame as well as flamelet regimes. For the latter, the strong coupling that exists between molecular diffusion and chemical reaction must be taken into account and this requires to improve the evaluation of both (i) the sub-grid mixing time scale, see for instance Mura et al. (2007) and Domingo et al. (2008) and (ii) the functional form of the micro-mixing model itself (Pope and Anand, 1984 ; Mura et al. 2003).

5. ACKNOWLEDGEMENTS

Fernando Oliveira de Andrade would like to thank CAPES and CNPq for the financial support during his doctorate activities at PUC-Rio and at the Laboratoire de Combustion et de Détonique de l'Université de Poitiers, France.

This work was performed while Luis Fernando Figueira da Silva was a Visiting Professor, funded by the National Petroleum Agency (Brazil), on leave from Centre National de la Recherche Scientifique, France.

6. REFERENCES

Besson, M., Bruel, P., Champion, J.L., Deshaies, B. 2000, "Experimental analysis of combusting flows developing over a plane-symmetric expansion", Journal of Thermophysics and Heat Transfer, 14(1):59-67.

Borghi, R., 1988, "On the Structure and Morphology of Turbulent Premixed Flames", Recent Advances in the Aaerospace Sciences, Edited by Corrado Casei, Plenum Publishing Corporation.

Colucci, P. J., Jaberi, F. A., Givi, P., Pope, S. B., 1998, "Filtered Density Function for Large Eddy Simulation of Turbulent Reacting Flows. Physics of Fluids, 10(2):499-515.

Domingo, P., Vervisch, L., Veynante D., 2008, "Large-Eddy Simulation of a lifted methane jet flame in a vitiated coflow", Combust. Flame, 152:415-432.

Ferziger, J., Peric, M., 2002, "Computational Methods for Fluid Dynamics", Third Edition, Ed. Springer Verlag, New York, USA.

Guilbert, N., Mura, A., Boust, B., Champion, M., "Study of premixed combustion instabilities using phase-locked tomography PIV", Proceedings of the 14th International Symposium on Applied Laser Techniques to Fluids Mechanics, Lisbon (Portugal) 7-10 July 2008.

Law, K. C., 2006, "Combustion Physics", Cambridge University Press, Chapter 1

Magre, P., Moreau P., Collin, G., Borghi, R., Pealat, M., 1988, "Further Studies by CARS of Premixed Turbulent Combustion in a High Velocity Flow", Combustion and Flame, 71:147-168.

Mura, A., Galzin, F., Borghi R., 2003, "A unified PDF-flamelet model for turbulent premixed combustion", Combust.Sci. Tech., 157:1573-1609.

Mura, A., Robin, V., Champion M., 2007, "Modeling of scalar dissipation in partially premixed turbulent flames", Combust. Flame, 149:217-224.

Peters, N., 2000, "Turbulent Combustion", Cambridge University Press, First Edition.

Pitsch H, 2006, "Large Eddy Simulation of Turbulent Combustion", Annual Review of Fluid Mechanics, 38:453-482.

Pope, S.B., Anand, M.S., 1984, "Flamelet and distributed combustion in premixed turbulent flames", Proc. Comb. Inst., 20:403-410.

Pope, S.B., 1985, "PDF methods for turbulent reactive flows", Prog. Energy Combust. Sci., 11:119-192.

Pope, S. B., 2000, "Turbulent Flows", Cambridge University Press, First Edition.

Smagorinski J., 1963, "General circulation experiments with the primitive equations, I: the basic experiment", Monthly Weather Review 91(3):99-164.

Villermaux, J., Falk, L., 1994, "A generalized mixing model for initial contacting of reactive fluids", Chemical Engineering Science, 49:5127-5140.

WEO 2008, "World Energy Outlook 2008", http://iea.org/weo/2008.asp